Simulation of Ultrafast All-Optical NOT Gate with Quantum-Dot SOA-Based Mach-Zehnder Switch

E. Dimitriadou* and K.E. Zoiros*
*Democritus University of Thrace, Department of Electrical and Computer Engineering, Xanthi, Greece
Email: {edimitr, kzoiros}@ee.duth.gr

***Abstract*—The feasibility of implementing an ultrafast NOT gate by means of a Mach-Zehnder switch that employs quantum-dot semiconductor optical amplifiers is theoretically investigated and demonstrated. The numerical simulation conducted for this purpose allows to find the permissible range of values for the critical parameters and a combination that is appropriate for realizing the specific Boolean function with high performance.**

I. INTRODUCTION

All-optical Boolean NOT logic is essential for all-optical signal processing as it is involved in many functionalities of fundamental and advanced level [1]. Given its significance it would be desirable if it could be realized at the increased single channel data rates aiming at coping with the unceasing bandwidth demand in modern networks [2]. The technology of quantum-dot (QD) SOAs is very promising for this purpose owing to its remarkably ultrafast response, which combined with its attractive characteristics distinguishes them from conventional SOAs [3]. Although QD-SOAs have been incorporated in the Mach-Zehnder interferometer (MZI) to achieve binary inversion [4], yet this has been done at the expense of having two intense pulse trains for controlling the switching of a third continuous wave signal. As a consequence the scheme is power consuming and complex to optimize, while the strain imposed on the SOA gain dynamics is heavy, which limits its overall practicality. Therefore in this paper we propose a more affordable way of executing the same task, which involves only two pulse trains and the MZI complementary output port. In this context we exploit in Section II a model that properly describes the operation of the employed configuration. The conducted simulation enables to assess the impact of the critical parameters on the defined performance metric and derive the allowable range of values for their selection so that the NOT gate functions with logical correctness and high quality, as detailed in Section III.

II. MODELLING

Fig. 1 depicts the block diagram of the simulated setup.

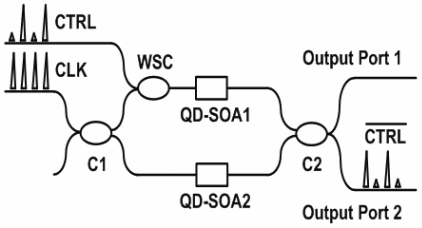

Figure 1. Simulated setup

The MZI has two synchronized inputs discriminated using different wavelengths in the 1550 nm region. These include the clock (CLK) that is held continuously to a logical '1' and the data-carrying control (CTRL) whose complement is mapped on the clock and transferred to output port 2 (O2) according to

$$P_{O2}(t)=\frac{1}{4}\left\{G_1(t)+G_2(t)+2\sqrt{G_1(t)G_2(t)}\cos\left[-\frac{\alpha}{2}\ln\left(\frac{G_1(t)}{G_2(t)}\right)\right]\right\}P_{CLK}(t) \quad (1)$$

where $P(t)$ demotes power, $G_1(t)$ and $G_2(t)$ are the gains experienced by the copies, in which the clock has been split by coupler C1, in the identical QD-SOAs 1 and 2, respectively, and $\alpha = 4.5$ is the alpha factor of the QD-SOAs. Since the control is inserted via a wavelength selective coupler (WSC) only in the upper arm of the MZI, this means that in the lower arm QD-SOA2 will be steadily operating in the small signal gain regime so that $G_2(t)=\exp\left[\left(g_{max}-\alpha_{int}\right)L\right]\sim 21$ dB for QD-SOA maximum modal gain, absorption coefficient and length $g_{max}=14\,cm^{-1}$, $\alpha_{int}=2\,cm^{-1}$ and $L=4$ mm, respectively. On the other hand $G_1(t)$ can be found from the wave propagation equation along the longitudinal, z, direction of QD-SOA1 [6] given by (2), in conjunction with the rate equations for the wetting layer (WL), excited state (ES) and ground state (GS) in (3), (4) and (5), respectively [5]

$$\frac{\partial S}{\partial z}=g_{\max}(2f-1)S-\alpha_{\text{int}}S \quad (2)$$

$$\frac{\partial N_w}{\partial t}=\frac{J}{eL_w}-\frac{N_w(1-h)}{\tau_{w2}}+\frac{N_Q h}{L_w\tau_{2w}}-\frac{N_w}{\tau_{wR}} \quad (3)$$

$$\frac{\partial h}{\partial t}=\frac{L_w N_w(1-h)}{N_Q\tau_{w2}}-\frac{h}{\tau_{2w}}-\frac{h(1-f)}{\tau_{21}}+\frac{f(1-h)}{\tau_{12}} \quad (4)$$

$$\frac{\partial f}{\partial t}=\frac{h(1-f)}{\tau_{21}}-\frac{f(1-h)}{\tau_{12}}-\frac{f^2}{\tau_{1R}}-\frac{g_{\max}(2f-1)L_w V_g}{N_Q}S \quad (5)$$

where t is time and $S = S(z, t)$, N_w, h and f are the control photon density, electron density in WL and electron occupation probabilities in the GS and ES, respectively, while the other QD-SOA structure parameters are defined and take values as in [6]. The set of coupled equations (2-5) is numerically solved for Gaussian-shaped pulses of width 1 ps using the 4th order Runge-Kutta method on a spatio-temporal grid to find $G_1(t) = S(L, t)/S(0, t)$ and replace it together with $G_2(t)$ in (1).

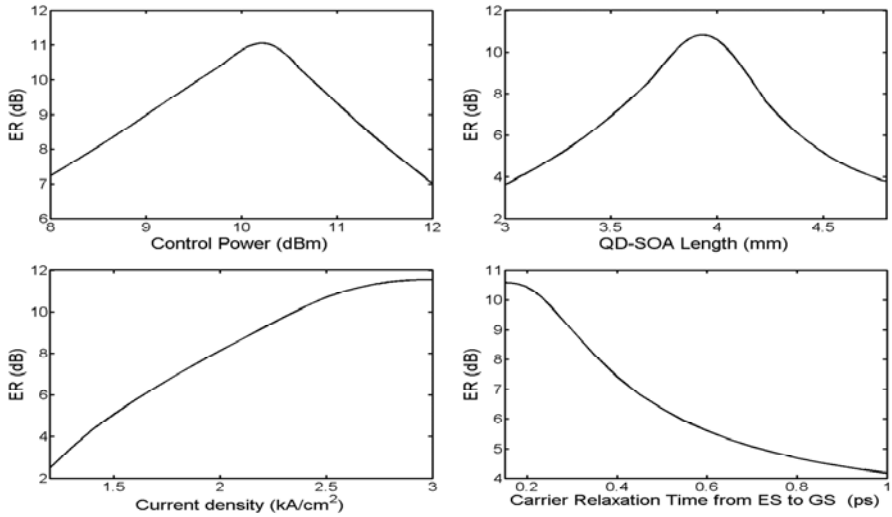

Figure 2. Extinction ratio (ER) variation vs. critical parameters

III. RESULTS

The performance of the scheme is evaluated at 160 Gb/s by means of the extinction ratio (ER) between the minimum and maximum peak power of the marks and spaces occurring at output port 2. This metric must be over 10 dB to ensure that the Boolean NOT operation is executed with high quality. In order to check if this requirement can be satisfied the ER variation against the critical parameters has been plotted in Fig. 2. More specifically, the ER curve has a bell-like shape in response to the change of the peak power of the control pulses and of the QD-SOAs length. This behaviour is attributed to the different intervals in which the phase difference induced by the control on the clock replicas takes values [1] as these parameters are altered, which in turn affects the magnitude of switching at output port 2 and hence the ER. Furthermore, the ER is improved with the increase of the injected current density, J, and after exceeding its defined minimum it becomes almost independent on this parameter because there is a redundancy of supplied carriers and the SOA is sufficiently biased to the desired point. Similarly the decrease of the carrier relaxation time from ES to GS, τ_{21}, ameliorates drastically the ER since the relevant dynamical process is accelerated and accordingly the '0's that occur at the considered output when the control is 'on' are suppressed to the same level more efficiently.

From the observation of Fig. 2 it can be deduced that the requirements for the critical parameters are 9.6 dBm $\leq P_{CTRL} \leq$ 10.7 dBm, 3.8 mm $\leq L \leq$ 4 mm, $J \geq 2.4$ kA/cm^2 and $\tau_{21} \leq 0.24$ ps. Thus by using the combination of values 10.5 dBm, 4 mm, 2.5 kA/cm^2 and 0.16 ps, respectively, a more than adequate ER of 10.75 dB can be obtained, which is reflected on the high quality of the pulse stream obtained at output port 2 (Fig. 3(b)) for the 8-bit-long data segment of 10111011 (Fig. 3(a)) inside the control 2^7-1 pseudorandom binary sequence. In contrast to the non-properly designed case (Fig. 3(c)), the marks have the same height, the spaces are nearly extinguished and the power emerges only at the time slots where a control pulse is absent, which is a key requirement for the achievement of correct logical inversion. Finally, it is noteworthy that with the specific selection of parameters the result of switching at output port 1 is also very good (Fig. 3(d)), which designates that the scheme can be exploited in the sophisticated applications for which the NOT gate is destined [1] with high overall performance.

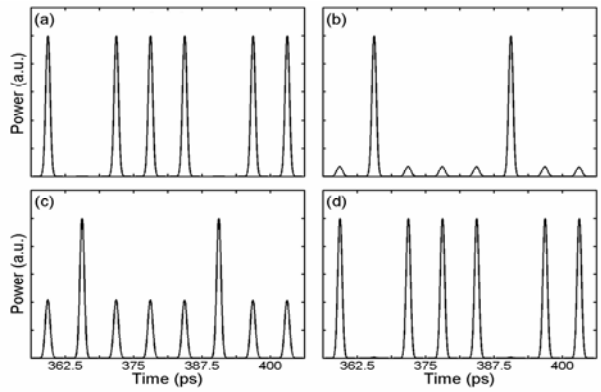

Figure 3. Simulation results

IV. CONCLUSION

The feasibility of realizing an ultrafast all-optical NOT gate with the QD-SOA-MZI operating in inverting mode has been theoretically demonstrated through numerical simulation, which has enabled to specify how the critical parameters must be selected to ensure logical correctness and high quality.

REFERENCES

[1] K.E. Zoiros, P. Avramidis, and C.S. Koukourlis, "Performance investigation of semiconductor optical amplifier-based ultrafast nonlinear interferometer in nontrivial switching mode," *Opt. Eng.*, vol. 47, pp. 115006/1-6, November 2008.

[2] A. Bogoni et al., "OTDM-based optical communications networks at 160 Gbit/s and beyond," *Opt. Fiber. Technol.*, vol. 13, pp. 1-12, January 2007.

[3] T.W. Berg and J. Mørk, "Saturation and noise properties of quantum-dot optical amplifiers," *IEEE J. Quantum Electron.*, vol. 40, pp. 1527-1539, November 2004.

[4] H. Sun, Q. Wang, H. Dong, and N.K. Dutta, "All-optical logic performance of quantum-dot semiconductor amplifier-based devices," *Microwave and Opt. Technol. Lett.*, vol. 48, pp. 29-35, January 2006.

[5] X. Li and G. Li, "Comments on "Theoretical analysis of gain recovery time and chirp in QD-SOA," *IEEE Photon. Technol. Lett.*, vol. 18, pp. 2434-2435, November 2006.

[6] A. Rostami, H.B.A. Nejad, R.M. Qartavol, and H.R. Saghai, "Tb/s optical logic gates based on quantum-dot semiconductor optical amplifiers," *IEEE J. Quantum Electron.*, vol. 46, pp. 354-360, March 2010.